

pubs.acs.org/est Article

# Brown Coal and Logwood Combustion in a Modern Heating Appliance: The Impact of Combustion Quality and Fuel on Organic Aerosol Composition

Patrick Martens, Hendryk Czech,\* Jürgen Orasche, Gülcin Abbaszade, Martin Sklorz, Bernhard Michalke, Jarkko Tissari, Tine Bizjak, Mika Ihalainen, Heikki Suhonen, Pasi Yli-Pirilä, Jorma Jokiniemi, Olli Sippula, and Ralf Zimmermann



**Cite This:** *Environ. Sci. Technol.* 2023, 57, 5532–5543



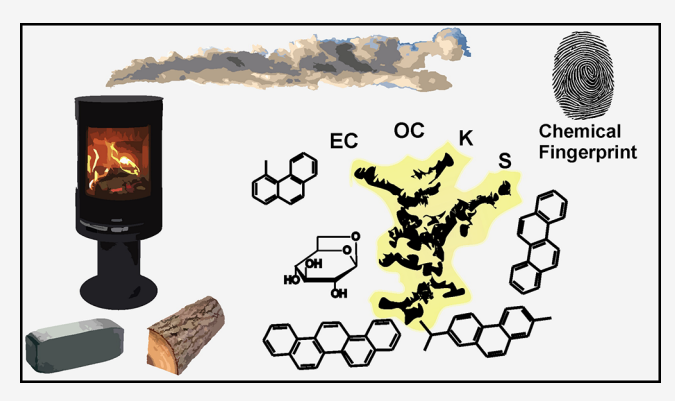
**ACCESS** 

III Metrics & More

Article Recommendations

s Supporting Information

ABSTRACT: Residential heating with solid fuels is one of the major drivers for poor air quality in Central and Eastern Europe, and coal is still one of the major fuels in countries, such as Poland, the Czech Republic, and Hungary. In this work, emissions from a single-room heater fueled with brown coal briquettes (BCBs) and spruce logs (SLs) were analyzed for signatures of inorganic as well as semivolatile aromatic and low-volatile organic constituents. High variations in organic carbon (OC) emissions of BCB emissions, ranging from 5 to 22 mg MJ<sup>-1</sup>, were associated to variations in carbon monoxide (CO) emissions, ranging from 900 to 1900 mg MJ<sup>-1</sup>. Residential BCB combustion turned out to be an equally important source of levoglucosan, an established biomass burning marker, as spruce logwood combustion, but



showed distinct higher ratios to manosan and galactosan. Signatures of polycyclic aromatic hydrocarbons emitted by BCB combustion exhibited defunctionalization and desubstitution with increasing combustion quality. Lastly, the concept of island and archipelago structural motifs adapted from petroleomics is used to describe the fraction low-volatile organic compounds in particulate emissions, where a transition from archipelago to island motifs in relation with decreasing CO emissions was observed in BCB emissions, while emissions from SL combustion exhibited the island motif.

KEYWORDS: photoionization, biomass burning, residential wood combustion, lignite, levoglucosan

#### **■** INTRODUCTION

Ambient air pollution by particulate matter (PM) has been shown to affect human health and the climate. 5-7 In Central and Eastern Europe, approximately 21 and 13% of outdoor PM<sub>2.5</sub> (particulate matter with an aerodynamic diameter smaller than 2.5  $\mu$ m) have been attributed to residential heating with solid fuels,8 and a reduction of PM<sub>2.5</sub> emissions from the residential and commercial sector is thought to reduce the pollution-related health burden in these regions. In particular, coal combustion in residential, small-scale heating appliances has been shown to pose a major burden to human health, having accounted for 10% of ambient PM<sub>2.5</sub> pollution but for 32% of pollution-related premature deaths in China in 2014. 10 Generally, toxicological responses in in vitro and in vivo studies have been shown to vary among residential heating appliances and solid fuels, 11,12 and differences in responses are thought to be caused by varying physical properties and chemical compositions of PM, <sup>13-16</sup> depending on the type of fuel, <sup>17-20</sup> type of appliance, <sup>18,20-23</sup> and combustion conditions. <sup>21,24-26</sup> Coal is still a commonly used fuel for residential heating in some areas of the world, such as China and Central and Eastern Europe. <sup>27</sup> In Europe, Poland, the Czech Republic, and Hungary still consume large quantities of coal for domestic heating, and consequently, residential coal combustion still is one of the largest contributors to overall poor air quality in these regions. <sup>28,29</sup> Leoni et al. <sup>29</sup> investigated the chemical composition of PM during a high-pollution episode with an average PM<sub>10</sub> of 47  $\mu$ g m<sup>3</sup> and peaks up to 286  $\mu$ g m<sup>3</sup> in a residential district of Ostrava, Czech Republic. Approximately 55% of ambient PM<sub>0.09-1.15</sub> was attributed to a mixture of secondary inorganic aerosol, biomass burning, and coal combustion. For the German–Czech border region, Schladitz

Received: November 22, 2022 Revised: March 16, 2023 Accepted: March 17, 2023 Published: March 28, 2023





et al.<sup>30</sup> apportioned 33 and 43% of ambient PM<sub>1</sub> to residential brown coal combustion on the German and Czech site during the heating period, respectively.

These source apportionment studies generally either rely on the availability of information on potential marker species<sup>3</sup> or comprehensive emissions profiles <sup>34,35</sup> as *a priori* information for Chemical Mass Balance or as a posteriori information for Positive Matrix Factorization models.<sup>36</sup> Markers are chemical species that can be traced back to precursor compounds in the fuel. In the past, cellulose and hemicelluloses as precursors for levoglucosan, manosan, and galactosan were thought to degrade in the early stages of coal diagenesis, 37,38 and thus, levoglucosan, manosan, and galactosan were primarily seen as markers for biomass burning. 31 Yet, evidence on the existence of cellulose and hemicelluloses in low-maturity coals is accumulating, 39-41 questioning the suitability of levoglucosan, manosan, and galactosan as markers. Moreover, the question arises whether there should be differences in signatures between biomass and coal in organic emissions. After all, coal originates from biomass, and molecular changes of the macromolecular fuel network upon maturation of coal are changing gradually from biomass to anthracite.<sup>38</sup> Emissions of low-maturity coals could be potential sources for species that are typically emitted from burning biofuels as well. Even very mature coals may emit anhydrous sugars at levels that may rival those from biomass combustion.4

For residential coal combustion emissions, molecular signatures of volatile organic compounds, 43-46 polycyclic aromatic hydrocarbons (PAHs), 47-49 and marker species<sup>32,42,50</sup> have been studied, but most of the information is limited to coal-appliance combinations representative for China. Especially, the existence and overall quantities of chemical markers depend on the type and rank of coal, the type of appliance, <sup>20,39</sup> and combustion conditions. Generally, the bulk of organic aerosol emissions originates from fuel pyrolysis upon ignition,<sup>51</sup> and signatures of organic pyrolysis products depend on conditions, such as temperature and heat rate. 52 Gao et al. 53 analyzed organic emissions from coal pyrolysis in a model reactor and found that relatively low temperatures (873 K) in their reactor yielded comprehensive aromatic emission profiles with O-containing PAHs, alkylated PAH, and arylic PAHs being equally abundant to unsubstituted PAHs. Increasing temperatures of their model reactor up to 1273 K led to a defunctionalization of aromatic organic compounds and a predominance of unsubstituted PAHs. Their findings imply that the molecular fingerprint of organic emissions from burning solid fuels depends strongly on the temperature regime under which the fuel was burned. Previous studies that focus on chemical fingerprints of marker species<sup>39-41</sup> may fall short in representing combustion appliances compliant with latest emission thresholds due to their rather simple setups, while studies that focus on emissions from coal combustion in modern appliances often do not go into depth regarding chemical fingerprints. 23,26,54,55

This study presents off-line and on-line analysis of aerosol emissions from low-maturity coal briquettes burned in a typical European, modern, nonheat retaining single-room heating appliance and evaluate biomass burning markers in the context of the continuum of coalification.

#### MATERIALS AND METHODS

**Combustion Appliance and Fuel.** Combustion experiments were carried out with a manually fired, nonheat-

retaining, single-room heating appliance (Figure S1, Aduro 9.3, Aduro A/S, Denmark) with a nominal output of 6 kW (Table S1), which is compliant with latest European legislation for emission regulation (EcoDesign 2022, effective January 1st, 2022). Given the compliance of the tested appliance with latest emission regulations, it is regarded a proxy for state-of-the-art, solid-fuel single-room heaters available in the European Union.

The fuels chosen for comparison are commercially available brown coal briquettes (BCBs, Rekord Briketts, Lausitz Energie Bergbau AG, Germany) and spruce logs (SLs, Picea abies). The briquettes were produced by drying and grinding of raw coal into 2.5 mm pieces and subsequent pressing into shape using high pressure without any additives. In comparison to biofuels, 56 the fuel composition of BCBs is characterized by a higher content of carbon and lower contents of hydrogen and oxygen (Table S2), resulting from loss of water and volatile matter upon coal maturation.<sup>38</sup> The structural changes in the macromolecular fuel network affect the combustion process, leading to a reduced fuel consumption rate, a reduction of the time the coal burns with a visible flame (homogeneous combustion of volatile components), and an extension of the time it does without a visible flame (heterogeneous combustion of char).<sup>56</sup> The Lusatian coal is a thermally immature, humic lignite, has formed in a low-lying reed-mire environment with few content of xylite (fossil wood remnants, mainly gymnosperms),<sup>57</sup> and is of high grade, i.e., low content of ash  $(<10\%^{58})$ . The sulfur content of 0.7% can be considered low.<sup>59</sup> The ash was analyzed by an external laboratory for selected inorganic constituents (Table S3) with known, inorganic pollutants, e.g., Pb, As, and Hg. Neither was found above the limits of quantification (LOQs).

**Combustion Procedure.** The combustion procedure used in this study has already been described in a previous study.<sup>19</sup> Briefly, combustion experiments were designed to cover a period of 4 h. Due to inherent differences, the ease of ignition and combustion rate, the mass of fuel, and the number of batches that were burned varied between both fuels. For SL experiments, one experiment comprised five consecutive batches of fuel with a weight of ca. 2 kg each, and each experiment started with the appliance being at room temperature. For BCB experiments, the combustion procedure comprised three batches with ca. 1.7 kg each. Because of the poor ease of ignition, the manufacturers from both the briquettes and stove recommend to burn at least one batch of wood prior to coal. In the present study, at least two batches of SLs were burned prior to BCBs to provide a sufficient bed of glowing ember for proper ignition of the BCBs. No emission samples were collected during these preparatory batches.

Exhaust Gas Measurements and Filter Sampling. The bulk flue gas composition (CO<sub>2</sub>, CO, H<sub>2</sub>O, SO<sub>2</sub>, and NO<sub>x</sub>) of entire combustion experiments, also comprising the batches of SLs prior to coal, was monitored from the undiluted flue gas by means of a Fourier-transform infrared spectrometer (DX4000, Gasmet Technologies Oy, Finland). The temperature was measured from the stack with a K-type thermocouple. PM<sub>2.5</sub> samples were taken over the 4 h combustion period, without preparatory batches in BCB experiments, using four channels of a modified filter sampler (Partisol 2300, Rupprecht & Patashnick, USA) with a flow rate 10 L min<sup>-1</sup> from diluted flue gas (DAS, Venacontra Oy, Finland). A dilution ratio of 30 was targeted for SL experiments, whereas dilution ratios of 60 for the first 10 min and 30 for the remaining 230 min of BCB experiments were targeted, respectively. At the beginning of

BCB experiments, a higher dilution was applied to reduce the exposure of rodents to CO in concurrent *in vivo* exposure experiments presented by Ihantola et al.  $^{12}$  and reduce potential carryover of organic species onto filters taken from BCBs. Analyses of organic compounds were performed from quartz fiber filters (47 mm diameter, 0.42 mm thickness, Munktell, Sweden), baked at 550  $^{\circ}$ C prior to sampling. For analyses of inorganic species, polytetrafluoroethylene filters (Zefluor, 1  $\mu$ m pore size, 47 mm diameter, Pall, USA) were used. Additionally, particle emissions and size distributions were monitored with a scanning mobility particle sizer (SMPS, model 3938, TSI Inc., USA) from a second dilution stage with an additional dilution ratio of 10. BCB and SL experiments were repeated nine and four times, respectively. On-line particle measurements are available for four experiments of both fuels each.

Targeted Chemical Analysis of Organic and Inorganic Compounds. Particle-bound organic species were analyzed by means of in situ derivatization (ID) thermal desorption (TD) gas chromatography (GC) time-of-flight (TOF) mass spectrometry (MS) with electron ionization.<sup>60</sup> Briefly, a filter aliquot was placed into the liner and rapidly heated to 300 °C to desorb organic species. In parallel, N-methyl-N-trimethylsilyl-trifluoroacetamide (MSTFA) was constantly added to the filter sample to derivatize polar compounds, preventing thermal decomposition. Identification and quantification were made based on retention time, similarity of mass spectra to NIST library entries, native and isotope-labeled standards of same or similar compounds. A variety of different polycyclic aromatic compounds (PACs), including 28 unsubstituted PAHs, 6 alkylated PAHs, 13 Oxy-PAHs, 3 aromatic Oheterocycles, as well as 3 resin acid derivatives, 3 anhydrous sugars, and 2 tetraphenyls (further specified in supplement, Table S7).

The inorganic composition was analyzed from PTFE filters by inductively coupled plasma atomic emission spectroscopy (ICP-AES; Optima 7300 DV, Perkin Elmer, Germany). Samples were digested with HNO<sub>3</sub> in a microwave system (Multiwave 3000, Anton Paar, Austria). Ultrapure water was added to yield 30 mL of solution. Details on instrument settings were presented earlier. <sup>12</sup> A full list of targeted elements is given in the supplement along with emission factors (Table S8).

Untargeted Analysis of Organic Compounds. The bulk carbonaceous particle fraction deposited on quartz fiber filters was analyzed by subjecting punches of 0.5 cm² to a thermal-optical carbon analysis (DRI 2001a, Atmoslytic Inc., USA), following the IMPROVE\_A protocol. Briefly, filter samples were stepwise heated in helium at temperatures of 140, 280, 480, and 580 °C and an oxidizing atmosphere of 98% helium and 2% oxygen at temperatures of 580, 740, and 840 °C. The optical correction was carried out by means of the reflectance signal of a 635 nm laser diode.

In addition to the targeted analysis of organic species, the carbon analyzer was coupled to a TOF-MS (Compact Reflectron Time-of-Flight Spectrometer II, Kaesdorf Geräte fuer Forschung and Industrie, Germany), and a fraction of the evolving gas portion was analyzed by means of resonance-enhanced multiphoton ionization (REMPI)<sup>63</sup> and single-photon ionization (SPI)<sup>64</sup> using 248 and 118 nm radiation, respectively. For REMPI, radiation from a KrF excimer laser (248 nm, 4.0 mJ/shot, shot frequency: 50 Hz, pulse duration: 5–15 ns, data acquisition rate 1 Hz, MLI-200, MLase AG, Germany) was used. For SPI, vacuum ultraviolet radiation of

118 nm was generated by tripling the third harmonic of a Nd:YAG solid-state laser (50 mJ/shot at third harmonic with 355 nm, shot frequency: 20 Hz, pulse duration: 5–7 ns, data acquisition rate 1 Hz, Spitlight 400, Innolas GmbH, Germany) in a gas cell filled with 4 mbar of xenon.

Data Processing and Evaluation. Calculations of emission factors and modified combustion efficiency (MCE) are described in the supplement. The calculations of emission factors have already been described in a previous study.<sup>65</sup> The MCE is an indicator for combustion quality, where combustion quality is high, i.e., complete oxidation of fuel to H2O and CO<sub>2</sub>, when MCE approaches unity. For statistical analysis, the Matlab Statistical Toolbox and Bioinformatics Toolbox (R2019b, The MathWorks Inc., Massachusetts, USA) was used. Results from statistical tests were considered significant at  $\alpha$  < 0.05. Statistical differences in means between both fuels were tested with the two-sided, nonparametric Mann-Whitney-U sum test, described in the supplement. Average emission factors for both fuels are presented as means ± standard deviations, which may be skewed by experiments with high emissions due to poor combustion quality.

#### ■ RESULTS AND DISCUSSION

Quality of Combustion and Particle Emission Characteristics. CO, an indicator for incomplete combustion conditions, was mainly emitted upon ignition of individual batches for both fuels and quickly declined to low levels for the majority of the combustion of a batch (Figure S2). Similarly, the MCE is low upon ignition of fuel and approaches unity a few minutes after. CO emissions averaged over the entire 4 h combustion cycle (Table S4) did not show significant differences between emissions from SL experiments with  $1000 \pm 150 \text{ mg MJ}^{-1}$  and BCB experiments with  $1300 \pm 270$ mg MJ<sup>-1</sup>. CO emissions from BCB burning however showed much greater variability between individual experiments; 4 h averages of individual experiments can be as just as low as wood combustion with approximately 900 mg MJ<sup>-1</sup> (Table S4, BCB2) but also approximately twice as high with 1900 mg MJ<sup>-1</sup> (BCB3). Furthermore, CO emissions from BCB burning seemed low when compared to EFs from other combinations of solid fuels and manually fueled heating appliances. 19 In SL experiments, a significant part of CO was emitted during the burn-off phase (secondary/tertiary air supplies closed and primary fully opened for shut-down of appliance) at the end of an experiment (Figure S2), whereas, in BCB experiments, this phase was not contributing largely to overall CO emissions. Thus, the difference in CO emissions between both fuels increases, with SL and BCB burning emitting on average 600  $\pm$ 100 and 1300  $\pm$  290 mg MJ<sup>-1</sup>, respectively (Table S4). When combustion quality is evaluated by means of MCE, significant differences were found between both fuels, both when the burn-off phase was omitted and when it was included. The absolute difference in MCE appears rather low with average MCE values of 0.976  $\pm$  0.004 for SL experiments and 0.965  $\pm$ 0.005 for BCB experiments. Similar to CO emissions, the difference in MCE between both fuels is increasing when the burn-off phase is omitted, but the absolute difference remains seemingly low with average MCE values of  $0.984 \pm 0.003$  for SL burning and 0.965  $\pm$  0.006 for BCB burning. In the following, CO emissions without the burn-off phase are used as indicators for combustion quality.

Particle number (PN) emissions and PN size distributions showed distinctive differences between both fuels (Figure S3,

Table S5). Total normalized PN concentrations were emitted on a much lower level from SL burning than from burning of BCBs with  $1.9 \pm 0.5 \times 10^{13}$  and  $23.7 \pm 5.1 \times 10^{13}$  MJ<sup>-1</sup>, respectively. In SL experiments, high PN concentrations were emitted with modes below 100 nm upon ignition of the fuel and quickly transitioned to modes above 100 nm in the flaming combustion phase. High PN emissions upon ignition of the fuel were only observed when a batch of SLs ignited comparatively slowly, suggesting that the duty cycle of the SMPS may be too slow to resolve quickly igniting batches of SLs appropriately. When flames extinguished, and the combustion transitioned to heterogeneous char combustion, comparatively high PN concentrations with modes below 100 nm were emitted. In BCB experiments, high PN concentrations with modes below 100 nm were observed upon ignition of a batch and subsequently transitioned to small particles with modes below 30 nm, which is close to the lower diameter limit of the instrument.

Total carbon (TC) accounted for the majority of the identified bulk  $PM_{2.5}$  from both fuels (Table S6), with emissions from BCBs of  $24\pm13$  mg C MJ $^{-1}$  being significantly lower than those from SLs with  $40\pm9.0$  mg C MJ $^{-1}$ . On average, OC emissions from BCB burning with  $15\pm10$  mg C MJ $^{-1}$  were not significantly higher than those from SLs with  $8.3\pm2.7$  mg C MJ $^{-1}$ , whereas EC emissions from BCB burning with  $8.7\pm4.2$  mg C MJ $^{-1}$  were significantly lower than emissions from SLs with  $33\pm11$  mg C MJ $^{-1}$ . BCB combustion is characterized by comparatively high OC/EC ratios ranging from 1.09 to 3.65, and the ratios seem to increase with increasing CO emissions (Figure 1). In

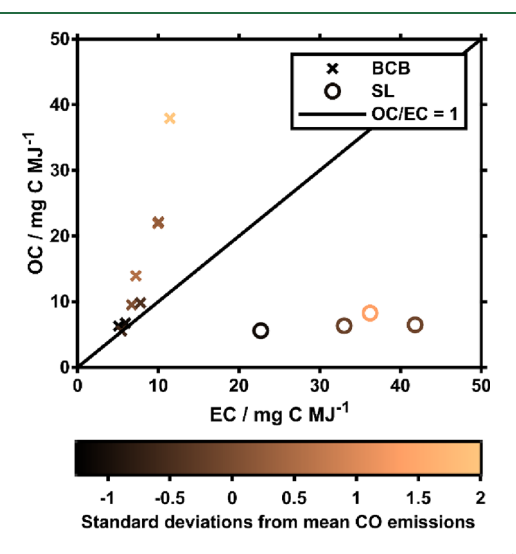


**Figure 1.** OC and EC emissions for brown coal briquettes (BCBs) and spruce logs (SL). To indicate the dependence of EC and OC on combustion quality, a color scale was added to denote the difference from average CO EFs in multiples of the standard deviation (SD) for each experiment. SL and BCB were standardized separately.

alignment with low variation in CO emissions, SL emissions were reproducible and characterized by low OC/EC ratios ranging from 0.16 to 0.25. High OC values found in BCB experiments were associated with high contributions of semi-volatile compounds found in OC1 and OC2 (Figure S4), ranging from 1.2 to 14.9 mg C MJ<sup>-1</sup> and 1.0 to 11.9 mg C MJ<sup>-1</sup>, respectively. OC3 and OC4, referring to low-volatile organic compounds, showed less variance in emissions ranging

from 1.1 to 6.7 mg C MJ<sup>-1</sup> and 2.2 to 4.4 mg C MJ<sup>-1</sup>, respectively. When CO emissions were low, individual OC fraction contributed roughly equally to overall OC, whereas when CO emissions were high, OC1 and OC2 accounted for the largest part of overall OC. In emissions from SL burning, there was little variance in individual OC fractions, and the individual OC fractions contributed approximately equally to overall OC. EC in BCB burning emissions consisted mostly of EC1, ranging from 4.7 to 9.8 mg MJ<sup>-1</sup>, while more refractory EC2 accounted for less EC with 0.1–0.8 mg C MJ<sup>-1</sup>, and EC3 was negligible. EC emissions from SL burning consisted predominantly of EC1, while both EC2 and EC3 were negligible.

These observations are in alignment with those made in many previous studies, which predominantly reported high OC/EC for  $coal^{66-72}$  and low ones for  $wood^{18,22,73-75}$ combustion. High EC emissions in SL experiments appear to be emitted continuously during flaming combustion with PN modes at approximately 100 nm. Because of high content of volatile matter in biofuels, SLs ignite fast and burn with a high rate resulting in large flames. Soot, including EC, is produced in the under-stoichiometric zones of the flames, and larger flames may have produced more soot, which is incompletely oxidized in the oxygen-rich area of the flame due to quenching by the stove casing. BCBs however ignite poorly and burn slowly because of comparatively low-volatile matter, leading to small flames that produced less soot and that were less affected by quenching. OC seems to be connected to high PN emissions and high CO emissions at the beginning of each batch with modes below 100 nm. The molecular composition of OC from BCB may have been stronger influenced by compounds that originate from fuel pyrolysis and evaporation occurring at the beginning of a batch, whereas OC from SL burning may be relatively enriched in species originating from incomplete combustion of soot intermediates being emitted throughout the combustion cycle similar to EC.

Higher Combustion Quality Leads to Defunctionalization and Desubstitution of Aromatic Compounds. Aromatic signatures of semi-volatile organic compounds were analyzed with REMPI during the fraction OC1-2 in the thermal-optical carbon analyzer. These fractions were combined because of the assumption that, within these two fractions, organic constituents mainly thermally desorb rather than degrade due to comparatively low temperatures in the thermal protocol.<sup>76</sup>

Aromatic signatures from BCB burning (Figure 2A,B) were generally more complex, i.e., many equally abundant signals, than those found in emissions from SL burning (Figure 2C). In SL emissions, the prominent signals can be tentatively assigned to common unsubstituted PACs (phenanthrene and anthracene: m/z 178; pyrene and fluoranthene: m/z 202; naphthobenzofurans: m/z 218; benzophenanthrenes and benzanthracenes: m/z 228; benzopyrenes and benzofluoranthenes: m/z 252), and these signals were also prominent in emissions from BCB. Moreover, emissions from BCB burning exhibited ion series of alkylated homologues (+14) for each of these parent ions, which were particularly intense in the experiment with high CO emissions (Figure 2A). In BCB experiments with low CO emission, these ion series were also found, but they were less abundant relative to the signals referring to the unsubstituted PACs, e.g., m/z 202 and 228 (Figure 2B). Phenanthrene/anthracene (m/z 178) and their alkylated homologues appeared to be the only series where the

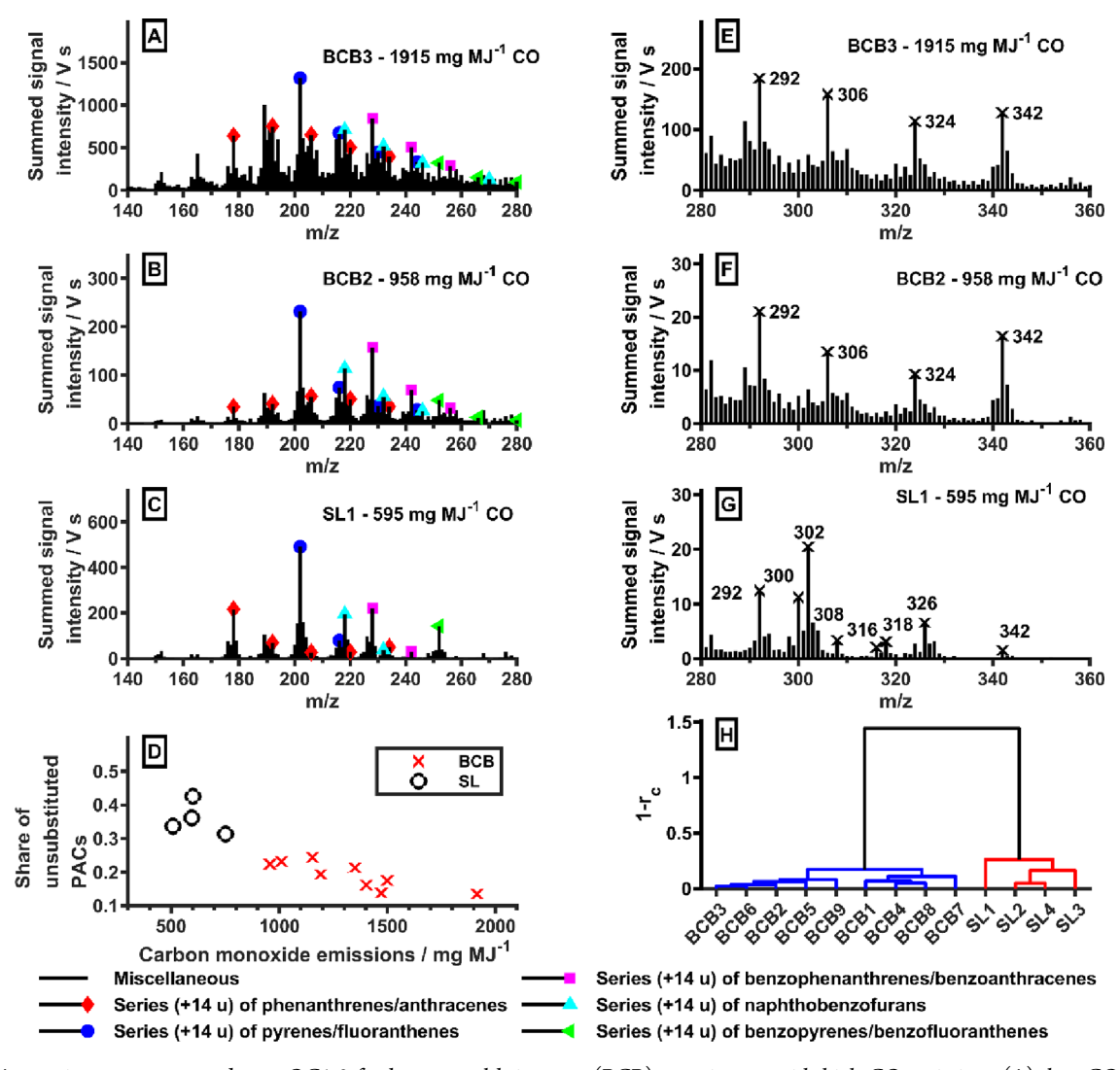


Figure 2. Aromatic pattern summed over OC1-2 for brown coal briquettes (BCB) experiments with high CO emissions (A), low CO emissions (B), and a spruce log (SL) experiment (C) with tentative assignment of alkylated series (+14) from polycyclic aromatic compounds (PACs). Panel D shows the share of unsubstituted PACs (m/z 178, 202, 218, 228, 252) from marked series (see legend) to the total signal in relationship with CO emission factors. Panels E, F, and G show the aromatic signature in the high-molecular-weight range, i.e., 280-350, summed from OC2 to 4 for the same experiments already shown in panels A, B, and C. Prominent peaks were used for hierarchical clustering of the fingerprint (H) using the uncentered correlation coefficient rc.

alkylated species (m/z 192, 206, 220, 234) were more than or equally intense to the unsubstituted parent. A similar pattern of alkylated phenanthrenes/anthracenes has already been observed for wood combustion (various wood types)<sup>22</sup> and is not distinctive for BCB burning. It seems that this series refers to an incremental dealkylation of organic resin acids, such as abietic acid.

Gao et al.  $^{53}$  demonstrated that emission profiles arising from combustion of coal in their model reactor are depending on combustion parameters, such as temperature and availability of oxygen, and high temperatures yield predominantly unsubstituted PACs at. Here, it was found that the contribution of the prominent unsubstituted PACs (m/z 178, 202, 218, 228, 252) to the total signal intensity increases with decreasing CO emission factors, indicating that changes in aromatic patterns are related to the differences in combustion quality. Lower CO emissions might have been associated with overall faster ignition, i.e., faster heat rates or higher temperatures upon fuel ignition within an experiment, which might have led to more pronounced cracking reactions in organics.  $^{77}$  Furthermore, this

might imply that wood combustion with less efficient stoves, unfavorable wood quality (e.g., high moisture, log size, etc.), or slow ignition<sup>22</sup> might similarly show an increase of substituted and functionalized aromatics because of poorer combustion quality due to a potential dependence of organic signatures on combustion quality.

Fingerprints of High-Molecular-Weight Species Can Be Used to Differentiate Brown Coal Briquettes and Spruce Logs. While the differences in the most intense features of the aromatic patterns were attributed to varying combustion quality, the fingerprint of high-molecular-weight compounds, i.e., m/z 280–400, revealed insights into biological markers (di- and triterpenoids) and their degradation products as well as higher molecular-weight PAHs, such as coronene. For this study, the scope is put on the m/z range from 280 to 350, although signals up to m/z 400 are known to occur in wood combustion-derived aerosol in OC2.<sup>22</sup>

Generally, high-molecular-weight species started occurring at the beginning of OC2. While some species evolve with comparatively sharp bell-shape profiles, others evolve with

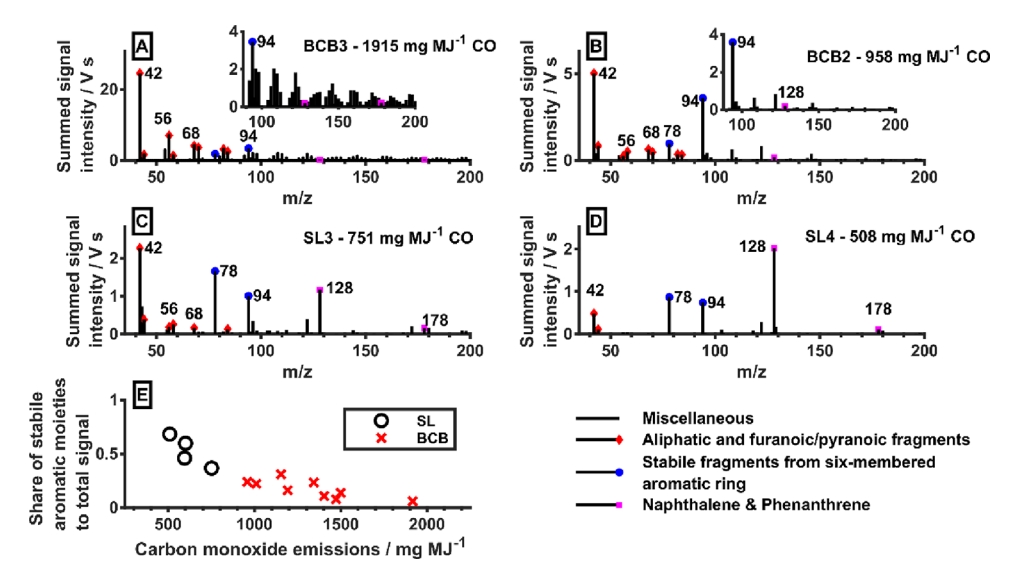


Figure 3. Mass spectra summed over OC3 and 4 for brown coal briquette (BCB) experiments with high and low CO emissions (A, B) and a spruce log (SL) experiments with relatively high and low emissions of CO (C, D) with a tentative assignment of signals to compound classes (legend). Panel E shows the increasing share of stabile aromatic moieties (benzene, phenol, naphthalene) in relationship to CO emissions.

broad, irregular shaped peaks (Figure S5). The former profile may refer to organic species that were already present in emissions and evaporate from the filter without thermal decomposition, whereas the latter may evolve due to pyrolysis of even larger compounds within the carbon analyzer or point to different desorption kinetics. Ion traces that show differences in their evolution profiles in the carbon analyzer may refer to different organic species in emissions from BCB and SL burning. For example, m/z 342 generally evolved with a sharp bell-shape profile at the beginning of OC2 in analysis runs of BCB emissions, even before lower weight species like m/z 324 and 306. In analysis runs of SL emissions, m/z 342 evolved slowly over the course of OC2 to OC4, and here, this m/z trace may rather refer to a compound, which is the result of analytical pyrolysis occurring in the carbon analyzer (Figure S5). Despite these difficulties in identifying compounds, this technique offers a rapid insight into a hardly accessible fraction of organic species.

In emissions from BCBs (Figure 2E,F), distinctive features were observed at m/z 342, 324, 306, and 292. All of these ions may refer a variety of picene-like compounds that are aromatic biomarkers known for coal combustion, e.g., various C<sub>4</sub>octahydropicenes (m/z 342), C<sub>3</sub>-tetrahydropicenes (m/z 324),  $C_2$ -picenes (m/z 306), and  $C_1$ -picene (m/z 292).<sup>32</sup> The difference in 18 u between these signals (342-324-306) may be explained by a loss of methane followed by a loss of H<sub>2</sub>, leading to incremental increases in aromatization. For SL, the most abundant signals are m/z 300, 302, and 326, and they may rather refer to larger PAH species, e.g., coronene and dibenzopyrenes among others, found in larger amounts in SL emissions in GC-MS analyses (Table S7). It seems likely that they could have formed by pyro synthesis as precursors of EC, with m/z 316, 318, and 342 possibly referring to the same species with an additional OH-group. All the aforementioned features can be used to get distinctive fingerprints that clearly differentiate both fuels (Figure 2J).

Low-Volatile Organics from Solid-Fuel Combustion: A Transition of Aromatic Archipelagos to Condensed PAH-Islands with Increasing Combustion Quality? Analytical pyrolysis is a common tool used to give insights into chemical structures of samples that are hardly accessible by conventional gas and liquid chromatography because of a low vapor pressure or poor solubility, e.g., chars from biomass and plastic pyrolysis  $^{78,79}$  or asphaltenes in crude oil.  $^{80,81}$  Organic species that have not evaporated up until the end of OC2 are characterized by a low vapor pressure, and they rather degrade thermally than evaporate in OC3 and OC4 (480 and 580 °C). This analytical pyrolysis induces a shift in mass evolving organic compounds from higher m/z ranges to low ones below m/z 100, and evolving species can be analyzed with a SPI-TOF-MS.  $^{76}$ 

For BCB emissions, it was found that the evolving patterns of low molecular species resulting from analytical pyrolysis in OC3 and OC4 changed substantially with varying CO emissions. In BCB experiments with high CO emissions (Figure 3A), aliphatic and/or furanoic signals accounted for the largest fractions of the mass spectrum (propene: m/z 42, butadiene m/z 56, etc.), and a complex pattern was found in the range of m/z 100-150 with signals that likely refer to substituted phenolic compounds. Thermally stabile sixmembered aromatic ring fragments (benzene, m/z 78; phenol, m/z 94) as well as larger PAHs, such as naphthalene (m/z128) and phenanthrene/anthracene (m/z 178), were either low in abundance or completely absent. When CO emissions were low (Figure 3B), the content of aliphatic/furanoic species decreased, while benzene and phenol emerged with higher abundance. Furthermore, only few substituted phenolic species were found with rather low intensity. In the SL experiment with relatively high CO emissions (Figure 3C), benzene and phenol accounted for the largest portion of the total signal intensity, while the signals of aliphatic/furanoic moieties were comparatively small. Naphthalene was the third most abundant fragment. Emissions of the SL experiment with the lowest CO emissions (Figure 3D) were comprised almost entirely of benzene, phenol, and naphthalene, while signals from aliphatic constituents were almost absent. Based on these observations, the increasing contribution of stabile aromatic moieties (benzene, phenol, naphthalene) was summed over OC 3 and 4 for each experiment and plotted in relationship to the CO emissions (Figure 3E). The share of aromatic moieties appears

Table 1. Emissions of Compound Classes Targeted with GC-MS in  $\mu$ g MJ<sup>-1</sup>a

	spruce logs				brown coal briquettes						
compound class	1	2	3	4	1	2	3	4	5	7	9
O-heterocycles	12	12	19	7.1	6.2	4.5	45	11	10	2.3	31
Oxy-PAH	500	480	570	310	250	140	990	330	230	140	730
alk-PAH	4.6	3.2	10	4.2	5.5	4.2	82	12	20	2.3	39
anhydrous sugar	150	59	380	5.7	70	120	580	100	170	29	210
unsubstituted PAH	180	190	480	160	97	55	530	140	130	41	360
resin acids derivatives	1.6	1.5	11	0.58	1.8	1.2	16	2.8	8.5	1.1	8.4
tetraphenyls	b.d.l	b.d.l	b.d.l	b.d.l	3	1.1	44	3.8	16	0.67	22
<sup>a</sup> Data for BCB 6 and 8 is not available.											

to increase in emissions from BCB to SL with decreasing CO

emission, indicating increasing graphitization of low-volatile organic species.

To improve the understanding of these findings, it is

To improve the understanding of these findings, it is necessary to introduce concepts native to other fields of research, i.e., petroleomics. 80,82 Similar to the chemical structure of asphaltenes, the chemical structure of the lowvolatile organics might be explained by two different models, the archipelago and island model. The archipelago motif resembles the macromolecular structure of lignin, where sixmembered aromatic rings are connected via aliphatic bridges varying in size. Low-volatile organic compounds might be lignin-like oligomers resulting of fragmentation of lignin and similar constituents in coal and biomass. In the island model, the organic compounds are made up of larger PAH-like islands with only few substituents in the periphery of an aromatic core. High content of aliphatic and substituted phenolic moieties in BCB experiment with elevated CO emissions points toward a higher abundance of organic structures with an archipelago motif. With increasing combustion quality and decreasing CO emissions in BCB experiments, the abundance of aliphatic and substituted phenolic moieties decreases, and unsubstituted units of benzene and phenol indicate a loss of aliphatic bridges between these archipelagos. With even higher combustion quality and decreasing CO emissions, as it is found in SL experiments, aliphatic moieties are even less abundant, and aromatic archipelagos seem to fuse to larger PAH-like islands, as suggested by the elevated abundance of naphthalene moieties. The lack of an overlap in data between SL and BCB experiments in terms of CO emissions is a limiting factor for the interpretation of these findings since it remains uncertain how comparable low-volatile organics were if CO emissions were identical. Furthermore, it remains uncertain how soot intermediates potentially formed during flaming combustion in SL experiments have influenced the composition. Nevertheless, the trend of increasing stabile aromatic moieties with decreasing CO emissions suggests that lowvolatility organics may transition from aromatic archipelagos to PAH-like islands with increasing combustion quality.

Residential Coal Combustion May Be a Source of Anhydrous Sugars. For a long time, cellulose and hemicellulose were thought to degrade in the initial stages of coal maturation,<sup>38</sup> but information on the presence of cellulose and hemicelluloses in Miocene lignites is accumulating.<sup>39–41,83</sup> These studies however either use purely pyrolytic methods or use simple burning setups that might not accurately represent burning conditions that are found in common residential heating appliances. For example, Rybicki et al.<sup>39</sup> used a simple burning setup by burning 50 g portions of Polish lignites in a crucible and sampled the evolving smoke. It remains unclear to

what extent their findings are influenced by low temperatures in small-scale setups in their experiments, how this has influenced ratios of levoglucosan to manosan and galactosan, and at what overall levels emissions can be expected in realworld combustion appliances. Yan et al.<sup>42</sup> demonstrated that semianthracite coal may emit a variety of different anhydrous sugars, with the dominant one being levoglucosan at levels of up to 12 mg kg<sup>-1</sup> (corresponding to ca. 480  $\mu$ g MJ<sup>-1</sup> with an assumed heating value of 25 MJ kg<sup>-1</sup>). <sup>56</sup> Levoglucosan emissions from coal combustion were outrivaled by bio fuels, which emitted roughly 1-3 orders of magnitude more on a per kg fuel burned basis. Ratios of levoglucosan to manosan and galactosan in coal emissions, ranging from 5 to 10 for both isomers, were rather low in comparison to biomass, ranging from 10 to 30 and 10 to 40 for levoglucosan-manosan and levoglucosan-galactosan ratios, respectively. In the comparison of a low-rank coal and spruce logwood in a real-world heating appliance, emissions of anhydrous sugars were found in comparable ranges of 5-380  $\mu$ g MJ<sup>-1</sup> in emissions from SL burning and 29-580  $\mu$ g MJ<sup>-1</sup> in emissions from BCB burning (Table 1). These levels are similar to those found in previous research with an average of 53, 72, and 110  $\mu$ g MJ<sup>-1</sup> for residential combustion of spruce, birch, and beech logwood.<sup>22</sup> Hence, low-maturity coals may be an equal emitter of these supposed markers for biomass combustion. For spruce combustion, levoglucosan as well as manosan and galactosan was found in each sample, and the ratios of levoglucosan to galactosan and manosan ranged from 6 to 20. In emissions from BCB burning, manosan was found in two samples in minor amounts of 2.9 and 0.17  $\mu g$  MJ<sup>-1</sup>, and galactosan was found in one sample with 0.029  $\mu g$  MJ<sup>-1</sup> (Table S8), which may point to a carryover from spruce batches burned prior to the coal. However, the Lusatian lignite deposits can be seen as extensions of Polish lignite deposits, 84 which have also showed traces of manosan and galactosan in emissions, 39-41 and thus, the presence of hemicellulose remnants in BCBs cannot be ruled out. The other samples from BCB burning generally showed no detectable amounts of galactosan and manosan, and hence, levoglucosan to galactosan and manosan ratios were very high, ranging from approximately  $3 \times 10^5 - 5 \times 10^6$  due to galactosan and manosan not being detectable (LOD/2 was assumed for both). The results demonstrate that anhydrous sugars and particularly levoglucosan are not unique to biomass burning but can also be emitted from burning of low-maturity coals in state-of-the art combustion appliances. Furthermore, these ratios can be used to constrain source apportionment

Emission Profiles of Metals and Metalloids from Burning of Low-Maturity Coal May Resemble Those of Wood Combustion. The sum of all elements quantified with ICP-AES ( $\Sigma E_{ICP-AES}$ ) was emitted at significantly different levels of 1.670  $\pm$  210  $\mu g$  MJ<sup>-1</sup> in SL experiments and 970  $\pm$ 170  $\mu$ g MJ<sup>-1</sup> in BCB experiments. In emissions from both fuels, K accounted for a large fraction of quantified inorganic species with 360  $\pm$  100 and 1040  $\pm$  140  $\mu g$  MJ<sup>-1</sup> in BCB and SL experiments, respectively, and a difference of factor 3 seem to be in good alignment with 4-fold higher fuel-K. However, K release does depend on the combustion temperature<sup>85</sup> and on the ternary ratio of  $(K_2O + Na_2O) / (CaO + MgO) / SiO_2$ due to competition among alkali and earth alkali metals for cationic positions in silicates, which are too low in volatility to be vaporized during combustion. 86 Neither for SL with a ratio of 7.80/43.16/1 nor for BCBs with 0.04/2.11/1, there is an excess of silicate, and for both of the fuels, there is a predominance of earth alkali metals over alkali metals indicating comparatively high release of K. Particle-bound S was the second major constituent and accounted for emission with 360  $\pm$  50 and 170  $\pm$  50  $\mu$ g MJ<sup>-1</sup> in BCB and SL experiments (both n = 4), respectively. A fold change of factor 2 is low given the 70-fold higher fuel-S in BCBs. The vast majority of fuel-S seems to remain in the ash. The sum of other targeted elements accounted for 230  $\pm$  40 and 430  $\pm$  80  $\mu$ g MJ<sup>-1</sup> in emissions BCBs and SLs, respectively. Out of 31 elements targeted, 12 (including S and K) were quantified at a noteworthy signal-noise ratio of 50 in either BCB or SL experiments (Figure S6). Emission factors of the majority of elements are in the same order of magnitude, which suggests that both fuels show only little differences. Na, Se, and As showed greater EFs in BCB emissions with 92  $\pm$  15, 0.73  $\pm$ 0.25, and 0.064  $\pm$  0.022  $\mu$ g MJ<sup>-1</sup> than in SL emissions with 7.1  $\pm$  1.3, 0.19  $\pm$  0.18, and 0.032  $\pm$  0.015  $\mu$ g MJ<sup>-1</sup>. As and Se were either <LOQ or not part of the fuel analysis (Table S2), technically not allowing a connection to the fuel content. However, As content in coals has been intensively studied and is typically associated with an exposure to marine bacteria.87 The world average for the As Clarke index of lignites is 7.4  $\pm$ 1.4 mg kg<sup>-1</sup>, <sup>87</sup> and therefore, the fuel-As of the Lusatian lignite with <0.8 mg kg<sup>-1</sup> can be regarded very low.<sup>22</sup> Burning of other Central European lignites with higher As content, e.g., from the northern Czech basin with a fuel-As content of 3245 mg kg<sup>-1,87</sup> likely results in much higher emissions. Se is typically found in high-sulfur coals because its ease of reduction leads to "Se-pumping" from oxidative into anoxic hydro sulfuric waters. <sup>88</sup> Accordingly, differences of factor 4 in EFs of Se between both fuels can be regarded small. High emissions of Na are typically associated with emissions from coal; however, emission factors of 92  $\pm$  15  $\mu$ g MJ<sup>-1</sup> from BCBs do not seem elevated in comparison to previously reported emission factors of 50 µg MJ<sup>-1</sup> for logwood combustion and 900 µg MJ<sup>-1</sup> for pellet combustion.<sup>22</sup> W, Cd, and Mn were found in greater amounts in SL emission with 3.2  $\pm$  0.6, 0.38  $\pm$ 0.12, and 3.9  $\pm$  2.4  $\mu$ g MJ<sup>-1</sup> than in BCB emissions with 0.2  $\pm$ 0.1,  $0.091 \pm 0.014$ , and  $0.955 \pm 0.700 \,\mu g \, MJ^{-1}$ . Concentration of the heavy metals cannot be traced back to the elemental composition of the fuel because they were either not targeted (W), <LOQ in both fuels (Cd), or found at similar levels (Mn). It is possible that it is the result of contamination of plants with heavy metals, resulting of pollution of soils by industry and a favorable environment for uptake (temperature, pH of soil, etc.). 89 Thus, EFs of these elements may not be representative for wood combustion in general but only for the region where the wood was lumbered. Inherently, emissions may depend on the choice of fuel (type of wood and coal), and

there may be coals that can be differentiated from wood by arsenic and selenium emissions or content of heavy metals. Nevertheless, the coal chosen here demonstrates that low-maturity coals may resemble wood profiles.

#### ASSOCIATED CONTENT

#### **Supporting Information**

The Supporting Information is available free of charge at https://pubs.acs.org/doi/10.1021/acs.est.2c08787.

Stove and fuel characterization (tables and figure); consumption of energy in the residential sector by fuel; description of calculations of emission factors and modified combustion efficiency and Mann—Whitney-U test; emissions of gaseous species (figure and data table) and emissions of particles via SMPS (figure & data table); emission factors of metals and metalloids (figure and table); and results from thermal-optical carbon analysis (table), evolution of high-molecular-weight species in thermal-optical carbon analysis (figure), and emissions of targeted organic compounds (table) (PDF)

#### AUTHOR INFORMATION

#### **Corresponding Author**

Hendryk Czech — Joint Mass Spectrometry Center (JMSC), Department of Analytical and Technical Chemistry, Institute of Chemistry, University of Rostock, Rostock D-18059, Germany; Joint Mass Spectrometry Center (JMSC), Comprehensive Molecular Analytics (CMA), Department Environmental Health, Helmholtz Zentrum München GmbH, Neuherberg D-85764, Germany; orcid.org/0000-0001-8377-4252; Phone: +49 381 498-6532; Email: hendryk.czech@uni-rostock.de; Fax: +49 381 498-118 6527

#### **Authors**

Patrick Martens – Joint Mass Spectrometry Center (JMSC), Department of Analytical and Technical Chemistry, Institute of Chemistry, University of Rostock, Rostock D-18059, Germany

Jürgen Orasche – Joint Mass Spectrometry Center (JMSC), Comprehensive Molecular Analytics (CMA), Department Environmental Health, Helmholtz Zentrum München GmbH, Neuherberg D-85764, Germany

Gülcin Abbaszade – Joint Mass Spectrometry Center (JMSC), Comprehensive Molecular Analytics (CMA), Department Environmental Health, Helmholtz Zentrum München GmbH, Neuherberg D-85764, Germany

Martin Sklorz – Joint Mass Spectrometry Center (JMSC), Comprehensive Molecular Analytics (CMA), Department Environmental Health, Helmholtz Zentrum München GmbH, Neuherberg D-85764, Germany

Bernhard Michalke — Research Unit Analytical BioGeoChemistry, Helmholtz Zentrum München GmbH, Neuherberg D-85764, Germany; orcid.org/0000-0001-6376-2588

Jarkko Tissari — Department of Environmental and Biological Sciences, University of Eastern Finland, Kuopio FI-70211, Finland

Tine Bizjak — Department of Environmental and Biological Sciences, University of Eastern Finland, Kuopio FI-70211, Finland; Present Address: Department of Environmental

- Sciences, Jozef Stefan Institute, Ljubljana SL-1000, Slovenia (T.B.); orcid.org/0000-0003-1276-4166
- Mika Ihalainen Department of Environmental and Biological Sciences, University of Eastern Finland, Kuopio FI-70211, Finland
- Heikki Suhonen Department of Environmental and Biological Sciences, University of Eastern Finland, Kuopio FI-70211, Finland
- Pasi Yli-Pirilä Department of Environmental and Biological Sciences, University of Eastern Finland, Kuopio FI-70211, Finland; orcid.org/0000-0002-7882-4574
- Jorma Jokiniemi Department of Environmental and Biological Sciences, University of Eastern Finland, Kuopio FI-70211, Finland
- Olli Sippula Department of Environmental and Biological Sciences, University of Eastern Finland, Kuopio FI-70211, Finland; Department of Chemistry, University of Eastern Finland, Joensuu FI-80101, Finland; orcid.org/0000-0002-6981-2694
- Ralf Zimmermann Joint Mass Spectrometry Center (JMSC), Department of Analytical and Technical Chemistry, Institute of Chemistry, University of Rostock, Rostock D-18059, Germany; Joint Mass Spectrometry Center (JMSC), Comprehensive Molecular Analytics (CMA), Department Environmental Health, Helmholtz Zentrum München GmbH, Neuherberg D-85764, Germany

Complete contact information is available at: https://pubs.acs.org/10.1021/acs.est.2c08787

#### **Notes**

The authors declare no competing financial interest.

#### ■ ACKNOWLEDGMENTS

The authors acknowledge the support by the Helmholtz Association of German Research Centres (HGF) within the Helmholtz International Lab aeroHEALTH (Interlabs-0005) and Helmholtz Virtual Institute of Complex Molecular Systems in Environmental Health (HICE), and the Academy of Finland (grant no. 304459).

#### REFERENCES

- (1) Brunekreef, B.; Holgate, S. T. Air pollution and health. *Lancet* 2002, 360, 1233-1242.
- (2) Shiraiwa, M.; Ueda, K.; Pozzer, A.; Lammel, G.; Kampf, C. J.; Fushimi, A.; Enami, S.; Arangio, A. M.; Fröhlich-Nowoisky, J.; Fujitani, Y.; Furuyama, A.; Lakey, P. S. J.; Lelieveld, J.; Lucas, K.; Morino, Y.; Pöschl, U.; Takahama, S.; Takami, A.; Tong, H.; Weber, B.; Yoshino, A.; Sato, K. Aerosol Health Effects from Molecular to Global Scales. *Environ. Sci. Technol.* **2017**, *51*, 13545–13567.
- (3) Hamanaka, R. B.; Mutlu, G. M. Particulate Matter Air Pollution: Effects on the Cardiovascular System. Front. Endocrinol. 2018, 9, 680.
- (4) Cohen, A. J.; Brauer, M.; Burnett, R.; Anderson, H. R.; Frostad, J.; Estep, K.; Balakrishnan, K.; Brunekreef, B.; Dandona, L.; Dandona, R.; Feigin, V.; Freedman, G.; Hubbell, B.; Jobling, A.; Kan, H.; Knibbs, L.; Liu, Y.; Martin, R.; Morawska, L.; Pope, C. A., III; Shin, H.; Straif, K.; Shaddick, G.; Thomas, M.; van Dingenen, R.; van Donkelaar, A.; Vos, T.; Murray, C. J. L.; Forouzanfar, M. H. Estimates and 25-year trends of the global burden of disease attributable to ambient air pollution: an analysis of data from the Global Burden of Diseases Study 2015. *Lancet* 2017, 389, 1907—1918.
- (5) Bond, T. C.; Bergstrom, R. W. Light Absorption by Carbonaceous Particles: An Investigative Review. *Aerosol Sci. Technol.* **2006**, *40*, 27–67.

- (6) Yan, J.; Wang, X.; Gong, P.; Wang, C.; Cong, Z. Review of brown carbon aerosols: Recent progress and perspectives. *Sci. Total Environ.* **2018**, *634*, 1475–1485.
- (7) Liu, D.; Whitehead, J.; Alfarra, M. R.; Reyes-Villegas, E.; Spracklen, D. V.; Reddington, C. L.; Kong, S.; Williams, P. I.; Ting, Y.-C.; Haslett, S.; Taylor, J. W.; Flynn, M. J.; Morgan, W. T.; McFiggans, G.; Coe, H.; Allan, J. D. Black-carbon absorption enhancement in the atmosphere determined by particle mixing state. *Nat. Geosci.* **2017**, *10*, 184–188.
- (8) World Health Organization. Residential heating with wood and coal: Health impacts and policy options in Europe and North America; http://www.euro.who.int/de/publications/abstracts/residential-heating-with-wood-and-coal-health-impacts-and-policy-options-ineurope-and-north-america (accessed 2019-09-09).
- (9) Silva, R. A.; Adelman, Z.; Fry, M. M.; West, J. J. The Impact of Individual Anthropogenic Emissions Sectors on the Global Burden of Human Mortality due to Ambient Air Pollution. *Environ. Health Perspect.* **2016**, *124*, 1776–1784.
- (10) Yun, X.; Meng, W.; Xu, H.; Zhang, W.; Yu, X.; Shen, H.; Chen, Y.; Shen, G.; Ma, J.; Li, B.; Cheng, H.; Hu, J.; Tao, S. Coal Is Dirty, but Where It Is Burned Especially Matters. *Environ. Sci. Technol.* **2021**, *55*, 7316–7326.
- (11) Kanashova, T.; Sippula, O.; Oeder, S.; Streibel, T.; Passig, J.; Czech, H.; Kaoma, T.; Sapcariu, S. C.; Dilger, M.; Paur, H.-R.; Schlager, C.; Mülhopt, S.; Carsten, W.; Schmidt-Weber, C.; Traidl-Hofmann, C.; Michalke, B.; Krebs, T.; Karg, E.; Jakobi, G.; Scholtes, S.; Schnelle-Kreis, J.; Sklorz, M.; Orasche, J.; Müller, L.; Reda, A.; Rüger, C.; Neumann, A.; Abbaszade, G.; Radischat, C.; Hiller, K.; Grigonyte, J.; Kortelainen, M.; Kuuspalo, K.; Lamberg, H.; Leskinen, J.; Nuutinen, I.; Torvela, T.; Tissari, J.; Jalava, P.; Kasurinen, S.; Uski, O.; Hirvonen, M.-R.; Buters, J.; Dittmar, G.; Jokiniemi, J.; Zimmermann, R. Emissions from a modern log wood masonry heater and wood pellet boiler: Composition and biological impact on airliquid interface exposed human lung cancer cells. *J. Mol. Clin. Med.* 2018, 1, 23–25.
- (12) Ihantola, T.; Hirvonen, M.-R.; Ihalainen, M.; Hakkarainen, H.; Sippula, O.; Tissari, J.; Bauer, S.; Di Bucchianico, S.; Rastak, N.; Hartikainen, A.; Leskinen, J.; Yli-Pirilä, P.; Martikainen, M.-V.; Miettinen, M.; Suhonen, H.; Rönkkö, T. J.; Kortelainen, M.; Lamberg, H.; Czech, H.; Martens, P.; Orasche, J.; Michalke, B.; Yildirim, A. Ö.; Jokiniemi, J.; Zimmermann, R.; Jalava, P. I. Genotoxic and inflammatory effects of spruce and brown coal briquettes combustion aerosols on lung cells at the air-liquid interface. *Sci. Total Environ.* **2022**, *806*, 150489.
- (13) Valavanidis, A.; Fiotakis, K.; Vlachogianni, T. Airborne particulate matter and human health: toxicological assessment and importance of size and composition of particles for oxidative damage and carcinogenic mechanisms. *J. Environ. Sci. Health, Part C: Environ. Carcinog. Ecotoxicol. Rev.* 2008, 26, 339–362.
- (14) Pope, C. A., III; Dockery, D. W. Health effects of fine particulate air pollution: lines that connect. *J. Air Waste Manage. Assoc.* **2006**, *56*, 709–742.
- (15) Rohr, A. C.; Wyzga, R. E. Attributing health effects to individual particulate matter constituents. *Atmos. Environ.* **2012**, *62*, 130–152.
- (16) Kim, K.-H.; Kabir, E.; Kabir, S. A review on the human health impact of airborne particulate matter. *Environ. Int.* **2015**, *74*, 136–143.
- (17) Orasche, J.; Schnelle-Kreis, J.; Schön, C.; Hartmann, H.; Ruppert, H.; Arteaga-Salas, J. M.; Zimmermann, R. Comparison of Emissions from Wood Combustion. Part 2: Impact of Combustion Conditions on Emission Factors and Characteristics of Particle-Bound Organic Species and Polycyclic Aromatic Hydrocarbon (PAH)-Related Toxicological Potential. *Energy Fuels* **2013**, *27*, 1482–1491.
- (18) Orasche, J.; Seidel, T.; Hartmann, H.; Schnelle-Kreis, J.; Chow, J. C.; Ruppert, H.; Zimmermann, R. Comparison of Emissions from Wood Combustion. Part 1: Emission Factors and Characteristics from Different Small-Scale Residential Heating Appliances Considering Particulate Matter and Polycyclic Aromatic Hydrocarbon (PAH)-

- Related Toxicological Potential of Particle-Bound Organic Species. *Energy Fuels* **2012**, *26*, 6695–6704.
- (19) Martens, P.; Czech, H.; Tissari, J.; Ihalainen, M.; Suhonen, H.; Sklorz, M.; Jokiniemi, J.; Sippula, O.; Zimmermann, R. Emissions of Gases and Volatile Organic Compounds from Residential Heating: A Comparison of Brown Coal Briquettes and Logwood Combustion. *Energy Fuels* **2021**, 14010.
- (20) Křůmal, K.; Mikuška, P.; Horák, J.; Hopan, F.; Krpec, K. Comparison of emissions of gaseous and particulate pollutants from the combustion of biomass and coal in modern and old-type boilers used for residential heating in the Czech Republic, Central Europe. *Chemosphere* **2019**, 229, 51–59.
- (21) Bhattu, D.; Zotter, P.; Zhou, J.; Stefenelli, G.; Klein, F.; Bertrand, A.; Temime-Roussel, B.; Marchand, N.; Slowik, J. G.; Baltensperger, U.; Prévôt, A. S. H.; Nussbaumer, T.; El Haddad, I.; Dommen, J. Effect of Stove Technology and Combustion Conditions on Gas and Particulate Emissions from Residential Biomass Combustion. *Environ. Sci. Technol.* **2019**, *53*, 2209–2219.
- (22) Czech, H.; Miersch, T.; Orasche, J.; Abbaszade, G.; Sippula, O.; Tissari, J.; Michalke, B.; Schnelle-Kreis, J.; Streibel, T.; Jokiniemi, J.; Zimmermann, R. Chemical composition and speciation of particulate organic matter from modern residential small-scale wood combustion appliances. *Sci. Total Environ.* **2018**, *612*, *636*–648.
- (23) Horak, J.; Kubonova, L.; Krpec, K.; Hopan, F.; Kubesa, P.; Motyka, O.; Laciok, V.; Dej, M.; Ochodek, T.; Placha, D. PAH emissions from old and new types of domestic hot water boilers. *Environ. Pollut.* **2017**, 225, 31–39.
- (24) Elsasser, M.; Busch, C.; Orasche, J.; Schön, C.; Hartmann, H.; Schnelle-Kreis, J.; Zimmermann, R. Dynamic Changes of the Aerosol Composition and Concentration during Different Burning Phases of Wood Combustion. *Energy Fuels* **2013**, 27, 4959–4968.
- (25) Czech, H.; Sippula, O.; Kortelainen, M.; Tissari, J.; Radischat, C.; Passig, J.; Streibel, T.; Jokiniemi, J.; Zimmermann, R. On-line analysis of organic emissions from residential wood combustion with single-photon ionisation time-of-flight mass spectrometry (SPITOFMS). Fuel 2016, 177, 334–342.
- (26) Horák, J.; Laciok, V.; Krpec, K.; Hopan, F.; Dej, M.; Kubesa, P.; Ryšavý, J.; Molchanov, O.; Kuboňová, L. Influence of the type and output of domestic hot-water boilers and wood moisture on the production of fine and ultrafine particulate matter. *Atmos. Environ.* **2020**, 229, 117437.
- (27) Kerimray, A.; Rojas-Solórzano, L.; Amouei Torkmahalleh, M.; Hopke, P. K.; Ó Gallachóir, B. P. Coal use for residential heating: Patterns, health implications and lessons learned. *Energy Sustainable Dev.* **2017**, *40*, 19–30.
- (28) Junninen, H.; Mønster, J.; Rey, M.; Cancelinha, J.; Douglas, K.; Duane, M.; Forcina, V.; Müller, A.; Lagler, F.; Marelli, L.; Borowiak, A.; Niedzialek, J.; Paradiz, B.; Mira-Salama, D.; Jimenez, J.; Hansen, U.; Astorga, C.; Stanczyk, K.; Viana, M.; Querol, X.; Duvall, R. M.; Norris, G. A.; Tsakovski, S.; Wåhlin, P.; Horák, J.; Larsen, B. R. Quantifying the impact of residential heating on the urban air quality in a typical European coal combustion region. *Environ. Sci. Technol.* **2009**, *43*, 7964–7970.
- (29) Leoni, C.; Pokorná, P.; Hovorka, J.; Masiol, M.; Topinka, J.; Zhao, Y.; Křůmal, K.; Cliff, S.; Mikuška, P.; Hopke, P. K. Source apportionment of aerosol particles at a European air pollution hot spot using particle number size distributions and chemical composition. *Environ. Pollut.* **2018**, 234, 145–154.
- (30) Schladitz, A.; Leníček, J.; Beneš, I.; Kováč, M.; Skorkovský, J.; Soukup, A.; Jandlová, J.; Poulain, L.; Plachá, H.; Löschau, G.; Wiedensohler, A. Air quality in the German–Czech border region: A focus on harmful fractions of PM and ultrafine particles. *Atmos. Environ.* **2015**, 122, 236–249.
- (31) Simoneit, B. R. T. Biomass burning a review of organic tracers for smoke from incomplete combustion. *Appl. Geochem.* **2002**, 17, 129–162.
- (32) Oros, D. R.; Simoneit, B. R. T. Identification and emission rates of molecular tracers in coal smoke particulate matter. *Fuel* **2000**, *79*, 515–536.

- (33) Ramdahl, T. Retene-a molecular marker of wood combustion in ambient air. *Nature* **1983**, *306*, 580–582.
- (34) Galarneau, E. Source specificity and atmospheric processing of airborne PAHs: Implications for source apportionment. *Atmos. Environ.* **2008**, *42*, 8139–8149.
- (35) Tobiszewski, M.; Namieśnik, J. PAH diagnostic ratios for the identification of pollution emission sources. *Environ. Pollut.* **2012**, *162*, 110–119.
- (36) Hopke, P. K. Review of receptor modeling methods for source apportionment. J. Air Waste Manage. Assoc. 2016, 66, 237–259.
- (37) Hatcher, P. G.; Clifford, D. J. The organic geochemistry of coal: from plant materials to coal. *Org. Geochem.* **1997**, *27*, 251–274.
- (38) O'Keefe, J. M. K.; Bechtel, A.; Christanis, K.; Dai, S.; DiMichele, W. A.; Eble, C. F.; Esterle, J. S.; Mastalerz, M.; Raymond, A. L.; Valentim, B. V.; Wagner, N. J.; Ward, C. R.; Hower, J. C. On the fundamental difference between coal rank and coal type. *Int. J. Coal Geol.* **2013**, *118*, 58–87.
- (39) Rybicki, M.; Marynowski, L.; Simoneit, B. R. T. Composition of organic compounds from low-temperature burning of lignite and their application as tracers in ambient air. *Chemosphere* **2020**, *249*, 126087.
- (40) Marynowski, L.; Bucha, M.; Lempart-Drozd, M.; Stępień, M.; Kondratowicz, M.; Smolarek-Lach, J.; Rybicki, M.; Goryl, M.; Brocks, J.; Simoneit, B. R. T. Preservation of hemicellulose remnants in sedimentary organic matter. *Geochim. Cosmochim. Acta* **2021**, 310, 32–46.
- (41) Fabbri, D.; Torri, C.; Simoneit, B. R. T.; Marynowski, L.; Rushdi, A. I.; Fabiańska, M. J. Levoglucosan and other cellulose and lignin markers in emissions from burning of Miocene lignites. *Atmos. Environ.* **2009**, *43*, 2286–2295.
- (42) Yan, C.; Zheng, M.; Sullivan, A. P.; Shen, G.; Chen, Y.; Wang, S.; Zhao, B.; Cai, S.; Desyaterik, Y.; Li, X.; Zhou, T.; Gustafsson, Ö.; Collett, J. L., Jr. Residential Coal Combustion as a Source of Levoglucosan in China. *Environ. Sci. Technol.* **2018**, *52*, 1665–1674.
- (43) Tsai, S. M.; Zhang, J. J.; Smith, K. R.; Ma, Y.; Rasmussen, R. A.; Khalil, M. A. K. Characterization of non-methane hydrocarbons emitted from various cookstoves used in China. *Environ. Sci. Technol.* **2003**, *37*, 2869–2877.
- (44) Wang, Q.; Geng, C.; Lu, S.; Chen, W.; Shao, M. Emission factors of gaseous carbonaceous species from residential combustion of coal and crop residue briquettes. *Front. Environ. Sci. Eng.* **2013**, *7*, 66–76.
- (45) Zhang, J.; Smith, K. R.; Ma, Y.; Ye, S.; Jiang, F.; Qi, W.; Liu, P.; Khalil, M. A. K.; Rasmussen, R. A.; Thorneloe, S. A. Greenhouse gases and other airborne pollutants from household stoves in China: a database for emission factors. *Atmos. Environ.* **2000**, *34*, 4537–4549.
- (46) Zhang; Smith, K. R. Emissions of Carbonyl Compounds from Various Cookstoves in China. *Environ. Sci. Technol.* **1999**, 33, 2311–2320.
- (47) Wang, Y.; Xu, Y.; Chen, Y.; Tian, C.; Feng, Y.; Chen, T.; Li, J.; Zhang, G. Influence of different types of coals and stoves on the emissions of parent and oxygenated PAHs from residential coal combustion in China. *Environ. Pollut.* **2016**, 212, 1–8.
- (48) Zhang, Y.; Shen, Z.; Sun, J.; Zhang, L.; Zhang, B.; Zou, H.; Zhang, T.; Hang Ho, S. S.; Chang, X.; Xu, H.; Wang, T.; Cao, J. Parent, alkylated, oxygenated and nitrated polycyclic aromatic hydrocarbons in PM2.5 emitted from residential biomass burning and coal combustion: A novel database of 14 heating scenarios. *Environ. Pollut.* **2021**, 268, 115881.
- (49) Yang, X.; Liu, S.; Xu, Y.; Liu, Y.; Chen, L.; Tang, N.; Hayakawa, K. Emission factors of polycyclic and nitro-polycyclic aromatic hydrocarbons from residential combustion of coal and crop residue pellets. *Environ. Pollut.* **2017**, 231, 1265–1273.
- (50) Bi, X.; Simoneit, B. R. T.; Sheng, G.; Fu, J. Characterization of molecular markers in smoke from residential coal combustion in China. *Fuel* **2008**, *87*, 112–119.
- (51) Wang, X.; Cotter, E.; Iyer, K. N.; Fang, J.; Williams, B. J.; Biswas, P. Relationship between pyrolysis products and organic aerosols formed during coal combustion. *Proc. Combust. Inst.* **2015**, 35, 2347–2354.

- (52) Collard, F.-X.; Blin, J. A review on pyrolysis of biomass constituents: Mechanisms and composition of the products obtained from the conversion of cellulose, hemicelluloses and lignin. *Renewable Sustainable Energy Rev.* **2014**, *38*, 594–608.
- (53) Gao, S.; Zhang, Y.; Meng, J.; Shu, J. Real-time analysis of soot emissions from bituminous coal pyrolysis and combustion with a vacuum ultraviolet photoionization aerosol time-of-flight mass spectrometer. *Sci. Total Environ.* **2009**, 407, 1193–1199.
- (54) Šyc, M.; Horák, J.; Hopan, F.; Krpec, K.; Tomšej, T.; Ocelka, T.; Pekárek, V. Effect of Fuels and Domestic Heating Appliance Types on Emission Factors of Selected Organic Pollutants. *Environ. Sci. Technol.* **2011**, *45*, 9427–9434.
- (55) Krpec, K.; Horák, J.; Laciok, V.; Hopan, F.; Kubesa, P.; Lamberg, H.; Jokiniemi, J.; Tomšejová, Š. Impact of Boiler Type, Heat Output, and Combusted Fuel on Emission Factors for Gaseous and Particulate Pollutants. *Energy Fuels* **2016**, *30*, 8448–8456.
- (56) Vassilev, S. V.; Vassileva, C. G.; Vassilev, V. S. Advantages and disadvantages of composition and properties of biomass in comparison with coal: An overview. *Fuel* **2015**, *158*, 330–350.
- (57) Kus, J.; Dolezych, M.; Schneider, W.; Hofmann, T.; Visiné Rajczi, E. Coal petrological and xylotomical characterization of Miocene lignites and in-situ fossil tree stumps and trunks from Lusatia region, Germany: Palaeoenvironment and taphonomy assessment. *Int. J. Coal Geol.* **2020**, *217*, 103283.
- (58) Meshram, P.; Purohit, B. K.; Sinha, M. K.; Sahu, S. K.; Pandey, B. D. Demineralization of low grade coal A review. *Renewable Sustainable Energy Rev.* **2015**, *41*, 745–761.
- (59) Chou, C.-L. Sulfur in coals: A review of geochemistry and origins. *Int. J. Coal Geol.* **2012**, *100*, 1–13.
- (60) Orasche, J.; Schnelle-Kreis, J.; Abbaszade, G.; Zimmermann, R. Technical Note: In-situ derivatization thermal desorption GC-TOFMS for direct analysis of particle-bound non-polar and polar organic species. *Atmos. Chem. Phys.* **2011**, *11*, 8977–8993.
- (61) Chow, J. C.; Watson, J. G.; Chen, L.-W. A.; Chang, M. O.; Robinson, N. F.; Trimble, D.; Kohl, S. The IMPROVE\_A Temperature Protocol for Thermal/Optical Carbon Analysis: Maintaining Consistency with a Long-Term Database. *J. Air Waste Manage. Assoc.* **2007**, *57*, 1014–1023.
- (62) Chow, J. C.; Wang, X.; Sumlin, B. J.; Gronstal, S. B.; Chen, L.-W. A.; Trimble, D. L.; Kohl, S. D.; Mayorga, S. R.; Riggio, G.; Hurbain, P. R.; Johnson, M.; Zimmermann, R.; Watson, J. G. Optical Calibration and Equivalence of a Multiwavelength Thermal/Optical Carbon Analyzer. *Aerosol Air Qual. Res.* **2015**, *15*, 1145–1159.
- (63) Boesl, U. Laser mass spectrometry for environmental and industrial chemical trace analysis. *J. Mass Spectrom.* **2000**, 35, 289–304.
- (64) Hanley, L.; Zimmermann, R. Light and molecular ions: the emergence of vacuum UV single-photon ionization in MS. *Anal. Chem.* **2009**, *81*, 4174–4182.
- (65) Reda, A. A.; Czech, H.; Schnelle-Kreis, J.; Sippula, O.; Orasche, J.; Weggler, B.; Abbaszade, G.; Arteaga-Salas, J. M.; Kortelainen, M.; Tissari, J.; Jokiniemi, J.; Streibel, T.; Zimmermann, R. Analysis of Gas-Phase Carbonyl Compounds in Emissions from Modern Wood Combustion Appliances: Influence of Wood Type and Combustion Appliance. *Energy Fuels* **2015**, *29*, 3897–3907.
- (66) Chen, Y.; Zhi, G.; Feng, Y.; Liu, D.; Zhang, G.; Li, J.; Sheng, G.; Fu, J. Measurements of black and organic carbon emission factors for household coal combustion in China: implication for emission reduction. *Environ. Sci. Technol.* **2009**, *43*, 9495–9500.
- (67) Chen, Y.; Zhi, G.; Feng, Y.; Fu, J.; Feng, J.; Sheng, G.; Simoneit, B. R. T. Measurements of emission factors for primary carbonaceous particles from residential raw-coal combustion in China. *Geophys. Res. Lett.* **2006**, 33, L20815.
- (68) Chen, Y.; Sheng, G.; Bi, X.; Feng, Y.; Mai, B.; Fu, J. Emission factors for carbonaceous particles and polycyclic aromatic hydrocarbons from residential coal combustion in China. *Environ. Sci. Technol.* **2005**, *39*, 1861–1867.
- (69) Zhi, G.; Chen, Y.; Feng, Y.; Xiong, S.; Li, J.; Zhang, G.; Sheng, G.; Fu, J. Emission characteristics of carbonaceous particles from

- various residential coal-stoves in China. Environ. Sci. Technol. 2008, 42, 3310–3315.
- (70) Zhang, Y.; Schauer, J. J.; Zhang, Y.; Zeng, L.; Wei, Y.; Liu, Y.; Shao, M. Characteristics of particulate carbon emissions from real-world Chinese coal combustion. *Environ. Sci. Technol.* **2008**, 42, 5068–5073.
- (71) Shen, G.; Tao, S.; Chen, Y.; Zhang, Y.; Wei, S.; Xue, M.; Wang, B.; Wang, R.; Lu, Y.; Li, W.; Shen, H.; Huang, Y.; Chen, H. Emission characteristics for polycyclic aromatic hydrocarbons from solid fuels burned in domestic stoves in rural China. *Environ. Sci. Technol.* **2013**, 47, 14485–14494.
- (72) Shen, G.; Yang, Y.; Wang, W.; Tao, S.; Zhu, C.; Min, Y.; Xue, M.; Ding, J.; Wang, B.; Wang, R.; Shen, H.; Li, W.; Wang, X.; Russell, A. G. Emission factors of particulate matter and elemental carbon for crop residues and coals burned in typical household stoves in China. *Environ. Sci. Technol.* **2010**, *44*, 7157–7162.
- (73) Miersch, T.; Czech, H.; Hartikainen, A.; Ihalainen, M.; Orasche, J.; Abbaszade, G.; Tissari, J.; Streibel, T.; Jokiniemi, J.; Sippula, O.; Zimmermann, R. Impact of photochemical ageing on Polycyclic Aromatic Hydrocarbons (PAH) and oxygenated PAH (Oxy-PAH/OH-PAH) in logwood stove emissions. *Sci. Total Environ.* **2019**, *686*, 382–392.
- (74) Schmidl, C.; Luisser, M.; Padouvas, E.; Lasselsberger, L.; Rzaca, M.; Ramirez-Santa Cruz, C.; Handler, M.; Peng, G.; Bauer, H.; Puxbaum, H. Particulate and gaseous emissions from manually and automatically fired small scale combustion systems. *Atmos. Environ.* **2011**, *45*, 7443–7454.
- (75) Lamberg, H.; Sippula, O.; Tissari, J.; Jokiniemi, J. Effects of Air Staging and Load on Fine-Particle and Gaseous Emissions from a Small-Scale Pellet Boiler. *Energy Fuels* **2011**, *25*, 4952–4960.
- (76) Diab, J.; Streibel, T.; Cavalli, F.; Lee, S. C.; Saathoff, H.; Mamakos, A.; Chow, J. C.; Chen, L.-W. A.; Watson, J. G.; Sippula, O.; Zimmermann, R. Hyphenation of a EC / OC thermal—optical carbon analyzer to photo-ionization time-of-flight mass spectrometry: an off-line aerosol mass spectrometric approach for characterization of primary and secondary particulate matter. *Atmos. Meas. Tech.* **2015**, *8*, 3337–3353.
- (77) Morf, P.; Hasler, P.; Nussbaumer, T. Mechanisms and kinetics of homogeneous secondary reactions of tar from continuous pyrolysis of wood chips. *Fuel* **2002**, *81*, 843–853.
- (78) Friederici, L.; Meščeriakovė, S.-M.; Neumann, A.; Sermyagina, E.; Meščeriakovas, A.; Lähde, A.; Grimmer, C.; Streibel, T.; Rüger, C. P.; Zimmermann, R. Effect of hydrothermal carbonization and eutectic salt mixture (KCl/LiCl) on the pyrolysis of Kraft lignin as revealed by thermal analysis coupled to advanced high-resolution mass spectrometry. J. Anal. Appl. Pyrolysis 2022, 166, 105604.
- (79) Friederici, L.; Schneider, E.; Burnens, G.; Streibel, T.; Giusti, P.; Rüger, C. P.; Zimmermann, R. Comprehensive Chemical Description of Pyrolysis Chars from Low-Density Polyethylene by Thermal Analysis Hyphenated to Different Mass Spectrometric Approaches. *Energy Fuels* **2021**, *35*, 18185–18193.
- (80) Neumann, A.; Chacón-Patiño, M. L.; Rodgers, R. P.; Rüger, C. P.; Zimmermann, R. Investigation of Island/Single-Core- and Archipelago/Multicore-Enriched Asphaltenes and Their Solubility Fractions by Thermal Analysis Coupled with High-Resolution Fourier Transform Ion Cyclotron Resonance Mass Spectrometry. *Energy Fuels* **2021**, *35*, 3808–3824.
- (81) Rüger, C. P.; Neumann, A.; Kösling, P.; Vesga Martínez, S. J.; Chacón-Patiño, M. L.; Rodgers, R. P.; Zimmermann, R. Addressing Thermal Behavior and Molecular Architecture of Asphaltenes by a Thermal-Optical Carbon Analyzer Coupled to High-Resolution Mass Spectrometry. *Energy Fuels* **2022**, *36*, 10177–10190.
- (82) Chacón-Patiño, M. L.; Rowland, S. M.; Rodgers, R. P. Advances in Asphaltene Petroleomics. Part 1: Asphaltenes Are Composed of Abundant Island and Archipelago Structural Motifs. *Energy Fuels* **2017**, *31*, 13509–13518.
- (83) Fabbri, D.; Marynowski, L.; Fabiańska, M. J.; Zatoń, M.; Simoneit, B. R. T. Levoglucosan and other cellulose markers in

pyrolysates of Miocene lignites: geochemical and environmental implications. *Environ. Sci. Technol.* **2008**, *42*, 2957–2963.

- (84) Widera, M. Genetic classification of Polish lignite deposits: A review. *Int. J. Coal Geol.* **2016**, *158*, 107–118.
- (85) Sippula, O.; Lind, T.; Jokiniemi, J. Effects of chlorine and sulphur on particle formation in wood combustion performed in a laboratory scale reactor. *Fuel* **2008**, *87*, 2425–2436.
- (86) Sippula, O.; Lamberg, H.; Leskinen, J.; Tissari, J.; Jokiniemi, J. Emissions and ash behavior in a 500 kW pellet boiler operated with various blends of woody biomass and peat. *Fuel* **2017**, *202*, 144–153.
- (87) Yudovich, Y. E.; Ketris, M. P. Arsenic in coal: a review. *Int. J. Coal Geol.* **2005**, *61*, 141–196.
- (88) Yudovich, Y. E.; Ketris, M. P. Selenium in coal: A review. *Int. J. Coal Geol.* **2006**, *67*, 112–126.
- (89) Nagajyoti, P. C.; Lee, K. D.; Sreekanth, T. V. M. Heavy metals, occurrence and toxicity for plants: a review. *Environ. Chem. Lett.* **2010**, *8*, 199–216.

### ☐ Recommended by ACS

Mapping the Contribution of Biomass Burning to Persistent Organic Pollutants in the Air of the Indo-China Peninsula Based on a Passive Air Monitoring Network

Haoyu Jiang, Gan Zhang, et al.

JANUARY 19, 2023

ENVIRONMENTAL SCIENCE & TECHNOLOGY

READ 🗹

Carbonyl Emissions and Heating Temperatures across 75 Nominally Identical Electronic Nicotine Delivery System Products: Do Manufacturing Variations Drive Pulmonary...

Soha Talih, Alan Shihadeh, et al.

FEBRUARY 16, 2023

CHEMICAL RESEARCH IN TOXICOLOGY

READ 🗹

## **Size-Resolved Field Performance of Low-Cost Sensors for Particulate Matter Air Pollution**

Emilio Molina Rueda, John Volckens, et al.

FEBRUARY 08, 2023

ENVIRONMENTAL SCIENCE & TECHNOLOGY LETTERS

READ 🗹

Emission Characteristics and Formation Pathways of Intermediate Volatile Organic Compounds from Ocean-Going Vessels: Comparison of Engine Conditions and Fue...

Zeyu Liu, Jianmin Chen, et al.

SEPTEMBER 07, 2022

ENVIRONMENTAL SCIENCE & TECHNOLOGY

READ 🗹

Get More Suggestions >